JPhys Photonics

TOPICAL REVIEW • OPEN ACCESS

Optical polarization rogue waves and their identifications

To cite this article: Lei Gao *et al* 2020 *J. Phys. Photonics* **2** 032004

View the article online for updates and enhancements.

This content was downloaded from IP address 151.100.135.48 on 07/08/2020 at 15:40

IOP Publishing J. Phys. Photonics 2 (2020) 032004 https://doi.org/10.1088/2515-7647/ab9bf7

Journal of Physics: Photonics

CrossMark

OPEN ACCESS

RECEIVED
10 January 2020

REVISED
5 March 2020

ACCEPTED FOR PUBLICATION
11 June 2020

PUBLISHED
22 July 2020

Original content from this work may be used under the terms of the Creative Commons Attribution 4.0 licence.

Any further distribution of this work must maintain attribution to the author(s) and the title of the work, journal citation and DOI.

Topical Review

Optical polarization rogue waves and their identifications

Lei Gao[1], **Qiang Wu**[1], **Yulong Cao**[1], **Stefan Wabnitz**[2,3] **and Tao Zhu**[1]

[1] Key Laboratory of Optoelectronic Technology & Systems (Ministry of Education), Chongqing University, Chongqing 400044, People's Republic of China
[2] Dipartimento di Ingegneria dell'Informazione, Elettronica e Telecomunicazioni, Sapienza Università di Roma, Roma 00184, Italy
[3] Novosibirsk State University, 1 Pirogova str, Novosibirsk 630090, Russia

E-mail: gaolei@cqu.edu.cn

Keywords: laser, rogue waves, polarization, dissipative soliton, supercontinuum

Abstract

Optical rogue waves are a class of pulses with extremely large amplitudes, whose probability of occurrence unexpectedly deviates from Gaussian-law statistics. To date, the mechanisms of rogue wave generation are still debated: investigations are under way, exploring the statistics of various pulse dimensions across different physical domains. Although polarization is one of the fundamental parameters of optical rogue waves, its statistics have received little attention until recently. Here, we review recent process of the polarization-dependent properties of optical rogue waves in ultrafast optics. Based on a two-dimensional statistical model, we introduce the concept of optical polarization rogue waves. Specifically, we consider the frequency of generation of waves with freak or rogue state of polarization, with a probability of occurrence deviating from a normal distribution. We demonstrate three nonlinear optical laser systems: a partially mode-locked laser, a dissipative soliton laser, and supercontinuum generation within a highly nonlinear fiber. Further, we identify optical polarization rogue waves in nonlinear laser systems, and discuss their generation mechanisms. Related results reveal that optical polarization rogue waves are embedded in optical systems with a deteriorated degree of coherence, which originates from vector four-wave-mixing processes. Polarization-dependent investigations will provide additional insight for our understanding of optical rogue waves.

1. Introduction

1.1. Rogue waves

The concept of rogue waves (RWs) originates from oceanography. They are known as water waves with extremely large amplitude propagating in open oceans. Besides, these rare events emerge with unexpectedly large probabilities, which deviate from the power law wave amplitude statistics, and they leave without a trace [1–9]. These events lead to water waves as high as 30 m, which impose a great threat to ships and ocean liners, and even cause devastating damages. Motivated by the interest in their physics, and industrial applications, a huge amount of work has been carried out, to explore the origins and predictability of RWs. And some secrets behind RWs have been unveiled in recent groundbreaking research.

Experimentally, RWs can be identified by calculating probability density functions (PDFs): the presence of heavy-tailed statistics, typically L-shaped, which denotes the appearance of rogue events [10]. Several models have been developed, based on the weak nonlinear interactions between thousands of waves. Many of these models involve the nonlinear Schrödinger equation (NLSE): numerical simulations and analytical solutions such as coherent breathers or incoherent turbulence have been extensively compared. Various mechanisms generating RWs have been proposed so far: from the simple linear superpositions of random weak waves, to nonlinear effects such as modulation instability (MI) and breathers [11, 12]. For a physical system with low coherence, RWs within diverse parameters may occur across different dimensions [13–15]. Advanced investigations have been carried out, involving, e.g. three-dimensional RWs [16–18], higher-order or super RWs [19–21], and the resonant interaction of three waves [22]. However, the steep wave profile of

© 2020 The Author(s). Published by IOP Publishing Ltd

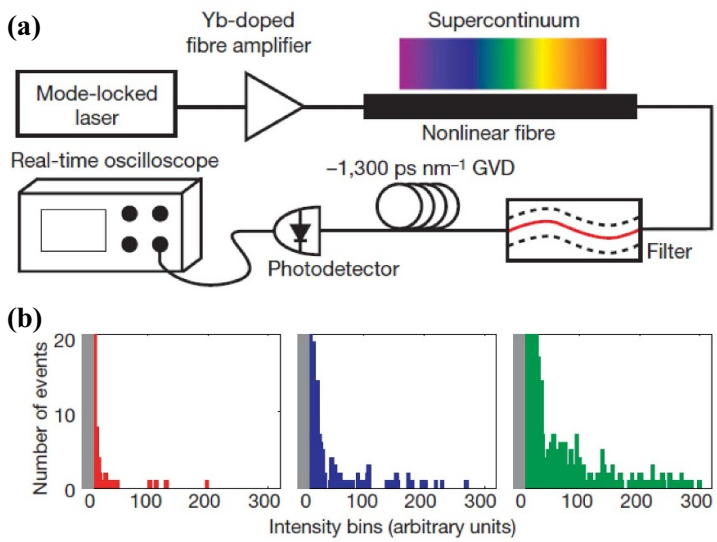

Figure 1.1. (a) Schematic of the experimental setup. (b) Histograms of filtered intensities for different average powers for the supercontinuum (reproduced from [24]).

extreme events often appears too freak to be fully captured. Many efforts have been devoted to the experimental observation of RWs in oceans and in the laboratory. The debate about the origin of RWs continues, and, in our opinion, it will remain standing as long as there will be discrepancies between theory and experiments.

1.2. Optical rogue waves

Given the harsh conditions, studying RWs in their natural oceanic environment is problematic. The observation of RWs has been extended to other domains. More examples are found in the fluence profiles of multi-filaments, supercontinuum generation (SCG) in optical fibers, Bose–Einstein condensates, electrostatic surface plasma, atmospheric waves, liquid helium, capillary waves, gravity wave trains and even in financial markets [23–38]. In 2007, due to phenomenological and physical analogies between extreme events in optics and hydrodynamics, the concept of optical RWs was introduced by D. R. Solli *et al*, based on long-tailed intensity histograms in the specifically filtered wavelength range of supercontinuum spectra [24]. As shown in figure 1.1, by using a real-time sepctrum detection based on dispersive Fourier transformation (DFT), they observed RWs in soliton-fission supercontinuum based on a micro-structured optical fiber. These results highlight the energy coupling between solitons and other wave packets, and the characteristic lifetimes during the formation of optical RWs.

Since then, great efforts have been devoted to finding examples of RWs in diverse optical systems, and different kinds of breathers or solitons have been proposed as the origin of optical RWs [25, 39–41]. Recently, highly developed real-time detection techniques, mainly based on the DFT and the time-lens, have been utilized to identify experimentally the presence of optical pulses with extremely high intensities. When a trough-to-crest height larger than 2 times the significant wave height (SWH) is found, the presence of RWs can be identified [42, 43]. Moreover, the occurrence of optical RWs can be identified, on the basis of diverse parameters across multiple dimensions. Examples include: pulse intensity [24], spectral width [44], spatial intensity in two-dimensions [23, 45], depth of dark pulses [46], and even rare pulses with right-skewed distributions [47]. The *rogueness* of a certain degree of freedom, rather than a *ultra-high value,* has been considered as a characteristic property of RWs. For a complete study of optical RWs, more parameters within other dimensions should be investigated further.

1.3. Interpretations for optical rogue waves

Recent years have witnessed a growing interest for optical RWs, while great debates on them are still ongoing in this community. In the pioneering works, the optical filtering technique has been taken seriously by several researchers, as a means to identify RWs [24, 27, 44]. Two different interpretations of optical RWs have been generally, although not completely, accepted. Both approaches involve two main phenomenological features of RWs. The first feature is the deviation of the statistics for the measured wave amplitude from the Gaussian behavior. The other one is the coherent build up of a RW in extended spatio-temporal systems. For optical fibers, the formation of RWs are determined mainly by the interplay between dispersion and

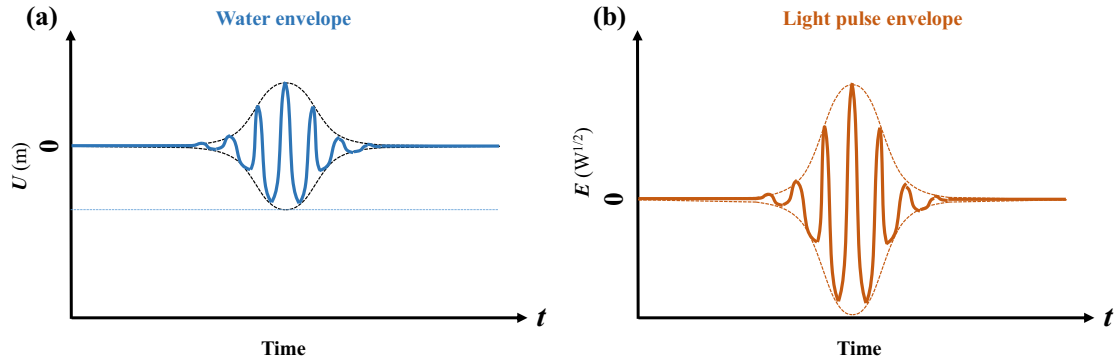

Figure 1.2. Wave evolution is described by the NLSE in two physical systems. (a) Soliton formed on the water. (b) Soliton formed in an optical fiber with anomalous dispersion.

nonlinearity, leading to the formation of time-frequency structures. While for spatially extended optical systems, two-dimensional structures are formed on the transverse wave front. Therefore, a reliable model for RWs should be described by partially differential equations, describing the action of dispersion and nonlinearity for the coherent build-up of giant waves [10]. On the other hand, we have to admit that the chaotic behavior or noise-induced intermittency, which can be described by ordinary differential equations, should to be considered for the classification of RWs [48]. The latter permit to describe the probability of RWs, which arises a fundamental question: the predictability of RWs. It was shown that RWs do not appear without a warning: they can preceded by a short phase of order [49–51]. Such a predictability can only be understood in terms of the language of turbulence [52–56].

A well-known theoretical model of RWs is provided by breather solutions of nonlinear optical systems. Such a model relies on the ocean-optics analogy. The dynamics of both ocean waves and pulses in optical fibers can be modeled by the same NLSE. For more complex systems, nonlinear wave dynamics involves an extended version of the Ginzburg-Landau equation. Figure 1.2 depicts wave evolution in the two physical systems, oceans and optical fibers. For optics, the NLSE describes the pulse envelope that modulates an electric field. While for hydrodynamics, the NLSE represents the envelope that modulates surface waves. Certain analogies do exist. Yet, such analogies should not be extended for different higher-order perturbations. The effect of perturbations on the solutions of the NLSE have been investigated [57]. It was found that RWs associated with first-order rational solution of the NLSE are robust against certain classes of perturbations.

An interesting phenomenon associated with RWs in optical fibers is the formation of breathers [58–60]. These highly coherent structures can be regarded as a kind of solitons on a finite background. These waves have certain analytical solutions. However it should be remembered that any real optical system is eventually dominated by linear loss. As a result of loss, a pure soliton is led out-of-balance by a mismatch between nonlinearity and dispersion. There are several kinds of breathers: the Akhmediev breathers, the Peregrine soliton, the Kuznetsov-Ma solitons. Higher-order strcutures are possible with stronger pulse localization and higher intensities. These breathers are frequently used for the interpretation of RWs, such as in MIs, in fiber resonators, or in SCG.

A great example is of RW generation mechanism is provided by MI. The nonlinear MI in optical fibers with anomalous dispersion is a simple and yet also complex nonlinear process [61, 62]. It is simple because the solutions representing the balance between nonlinearity and dispersion are simple and beautiful. However, noise-seeded nonlinear processes lead to fluctuations of the MI gain spectra. Besides, perturbations arising from higher-order dispersion and Raman scattering make breathers formed during the nonlinear MI process relatively hard to capture. Thanks to single-shot detection based on DFT, real time optical spectra for any number of round trips can be detected, and a certain evidence has been found of the links between breathers and optical RWs [63].

In spite of the success in interpreting RWs as coherent wave structures, based on either solitons or breathers, a debate still exists. This originates from the experimental observation of incoherent solitons, which were firstly found in photorefractive crystals [64]. Such solitons result from the spatial self-trapping of incoherent light in a nonlinear medium with high noninstantaneous response. When the response time is much larger than the correlation time of a beam, the field fluctuations are averaged by the photorefractive nonlinearity. Additional achievements have been made, e.g. MI of incoherent waves [65, 66], incoherent dark solitons [67], incoherent solitons in resonant interactions [68], and spectral incoherent solitons in optical

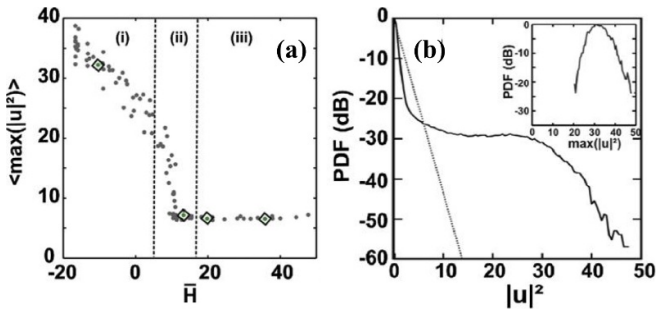

Figure 1.3. (a) Average of the maximum intensity peak as a function of the Hamiltonian H. (b) PDF of the field intensity, with the inset showing the PDF of the maxima of intensity (reproduced from [70]).

fibers [69]. Statistically, the kinetic wave theory can provide a nonequilibrium description of soliton dynamics.

Recent experiments provide other insights on the emergence of RWs in optical turbulence [70]. Figure 1.3 depicts the average of the maximum intensity peak as a function of wave energy H. Depending on the degree of incoherence, three regimes have been identified: coherent rogue quasi-solitons, intermittent-like rogue quasi-solitons, and sporadic RWs. The PDFs of waves in the three regimes are totally different. In the first regime (i), due to the large localization of power, the statistics deviate from the normal distribution, and high power quasi-soliton structures emerge. After that, the system operates in the second regime (ii), and an intermittent dynamics could be found, where quasi-solitons erratically appear and disappear. Indeed, the trajectory of quasi-solitons is not invisible. Besides, the long tail of the corresponding PDF can be attributed to the emergence of significant fluctuations. Next comes the third regime (iii), which is a fully incoherent regime. During this regime, there are no quasi-soliton structures, but sporadic extreme events can be found, although with small probabilities.

1.4. Polarization-dependent properties of RWs

The extensive experimental and theoretical investigations of optical RWs have been mostly focused on extreme events appearing in either the temporal or the spectral domains. Few studies have been carried out about extreme events in the polarization domain. Yet, as a fundamental parameter of light, the state of polarization (SOP) is of vital importance for any nonlinear optical process. In spite of that, most theoretical models of nonlinear optical process rely on a simple assumption of a fixed SOP. On the other hand, experimental results prove that oftentimes nonlinear optical processes are accompanied with an evolution of the SOP.

An experiment shown in figure 1.4 demonstrated polarization-dependent RWs dynamics in a fiber laser system without a saturable absorber (SA), based on an interaction mechanism involving a coupling between two polarization modes [71]. The cavity contains a 1480 nm laser diode, a pump polarization controller (PPoC), a 1480/1550 wavelength division multiplexer (WDM) before 1 m active fiber doped with Er^{3+}, a polarization controller and 614 m of single-mode fiber (SMF). Figure 1.4 (b) depicts the PDFs of the amplitudes of pulses on a logarithmic scale. A characteristic L-shaped distribution can be observed for the PDFs associated with different regimes: lonely patterns, twin patterns, three sisters patterns, cross and accelerated patterns.

In this experiment, the mechanism of interactions among the RWs, and different patterns does not primarily result from the nonlinearity in a passive fiber, as the pulse amplitudes are relatively low, but more likely from interactions in the active part, likely from polarization hole burning due to polarization attraction [72]. The occurrence of vector behavior was attributed to population inversion in the active fiber. As the pulse interactions are mutually exclusive, all the RW patterns are different manifestations of the same underlying process.

As discussed before, incoherent solitons also provide a platform to observe optical RWs [73]. Figure 1.5 depicts schematically a fiber ring laser cavity mode-locked by a semiconductor saturable absorber mirror (SESAM). The laser cavity includes an erbium-doped fiber (EDF) pumped by a 980 nm laser diode (LD), a polarization-insensitive circulator, a 980/1550 WDM, a polarization controller (PC). A polarization beam splitter (PBS) is used to investigate vector dynamics.

In this laser system, both polarization locking and polarization switching of incoherent solitons were observed. Figure 1.6 illustrates histograms for the x-polarization and the y-polarization of the detected single-shot spectra. As can be seen, both histograms exhibit long-tailed distributions. Waves with even four

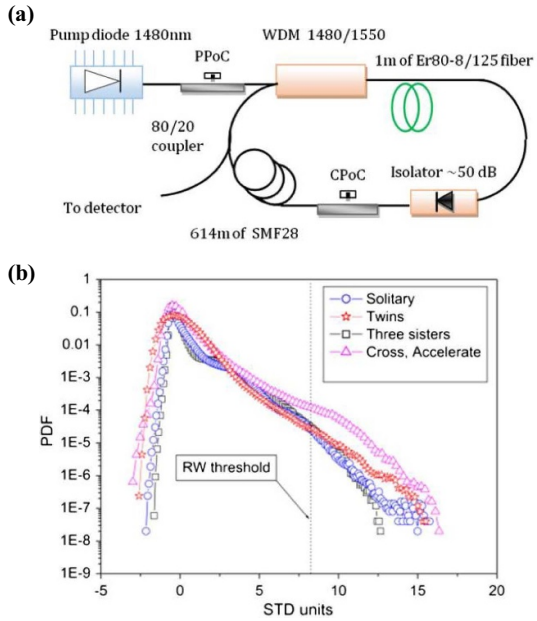

Figure 1.4. (a) Schematic of the fiber laser cavity. (b) PDFs of the pulse amplitudes for solitary, twins, three sisters and cross patterns (reproduced from [71]).

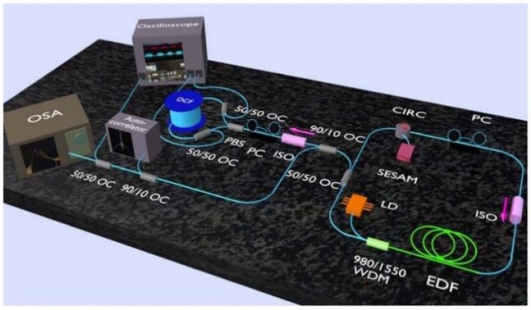

Figure 1.5. Schematic of a mode-locked fiber laser, and the measurement setup (reproduced from [73]).

times the SWH were found, which denotes the existence of extreme events. Besides, a great difference is shown in the two orthogonal polarization directions. The x-polarization is more likely to display explosive instabilities. Those results imply that optical RWs are polarization-dependent.

Despite the great achievements that have been made on polarization-resolved optical RWs, these do not represent RWs in the polarization domain, but rather temporal properties emerging in a specific SOP projection. At variance with the temporal or spatial RWs, we may introduce polarization rogue waves (PRWs) in the polarization domain, and be expressed give a new method for their idenfication. The SOP at a specific frequency (or wavelength) on the Poincaré sphere can as $\hat{S} = (s_1, s_2, s_3)$. Therefore, the relative distance, r, between two SOPs can be defined by

$$r = |S_m - S_n| = 2\sin^{-1}\left(\sqrt{(S_{m1} - S_{n1})^2 + (S_{m2} - S_{n2})^2 + (S_{m3} - S_{n3})^2}/2\right). \tag{1.1}$$

Based on this new parameter, r, we may investigate the polarization dynamics by calculating its probability distribution, and identify PRWs when the PDF of r is deviating from a normal distribution [74].

In the following sections, we will examine the statistical polarization distributions in three nonlinear optical systems, specifically: a partially mode-locked laser (PML), a dissipative soliton (DS) laser, and SCG. We identify the emergence of PRWs in all of these three laser systems, and discuss their generating mechanisms. In section 2 we shall discuss PRWs in PML, which undergo a coherence transition. Next, section 3 is devoted to exploring polarization evolutions during the build-up of DSs. PRWs are identified when the coherence is deteriorated by higher gain. Section 4 contains the experimental results on the PRWs

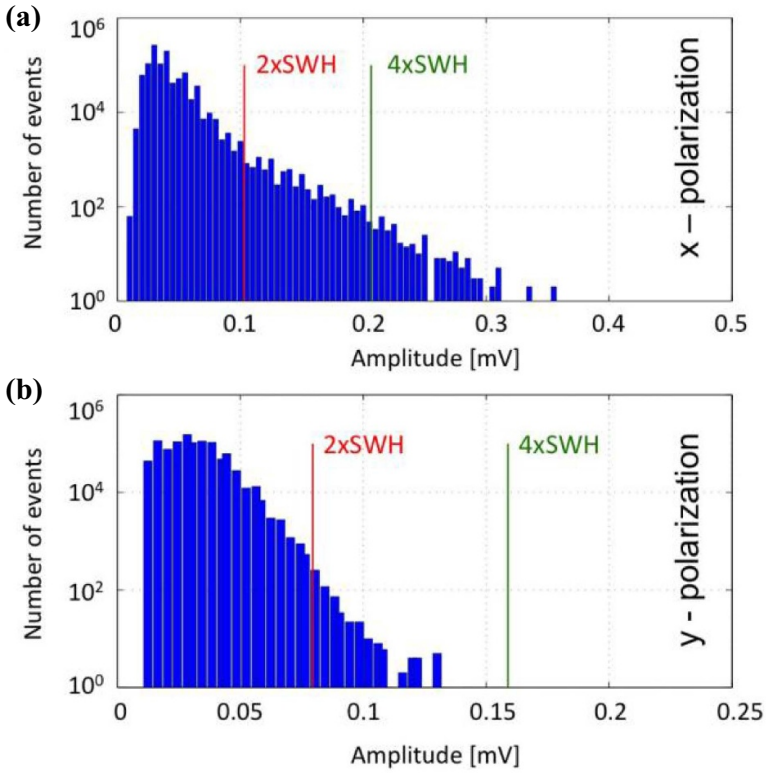

Figure 1.6. Histogram of the maximal spectral intensity fluctuations for (a) x-polarization and (b) y-polarization (reproduced from [73]).

in supercontinuum, based on a DS propagating in a zero-dispersion fiber. Finally, a short summary is given in section 5.

2. Optical polarization rogue waves in a PML

The coherence transition from high to low is common in many physical systems, where both stable coherent and low coherence structures can be observed [25, 70, 74 80]. Whereas, for a PML, spectral and temporal outputs are unstable. These outputs have also been called 'noise-like pulses', due to their appearance as noise-like bursts of radiation. Abundant works have been performed, revealing the existence of RWs in various laser systems [81, 82]. Here, we use the term of partially mode-locked laser with the emphasis of marking the difference with respect to the highly mode-locked lasers in section 3. Besides, the PML which is discussed here originates from a specific coherence-evolving mechanism: the generation of high coherent sidebands, and also to the presence of low-coherence nonlinear coupling processes. Primarily, energy transfers from a continuous wave (CW) central mode into parametric instability (PI) gain sidebands. PI is a special case of MI, where two pump photons at frequency of ω_0 are annihilated, and two new photons with Stokes or anti-Stokes frequencies are generated. As this degenerate four-wave-mixing (DFWM) process occurs within a cavity configuration, PI sidebands are highly coherent under the combined action of nonlinearity and periodic dispersion [64, 83–96]. The loss of coherence of PML is associated with cascaded vector mutual wave mixing of the PI sidebands within non-polarization-maintaining fibers, where bunches of pulses with irregular varying time duration and intensity are observed [97–100].

2.1. Experimental setup

The fiber cavity shown in figure 2.1(a) contains an EDF pumped by two CW lasers through two WDMs, SMF, dispersion compensating fiber (DCF), a polarization independent optical isolator (ISO), a PC, an optical coupler (OC), and a SA fabricated by filling reduced graphene oxide (rGO) flakes into cladding holes of a photonic crystal fiber (PCF), to provide enough nonlinear phase for mode-locking [101, 102]. Specifically, a high-speed polarization state analyzer (PSA) is utilized to detect the laser after filtering by a tunable filter (TF). In figure 2.1(b), the 100 single-shot spectra detected by DFT are consistent with the time-averaged optical spectrum. The full width at half maximum (FWHM) of the optical spectrum is 16 nm.

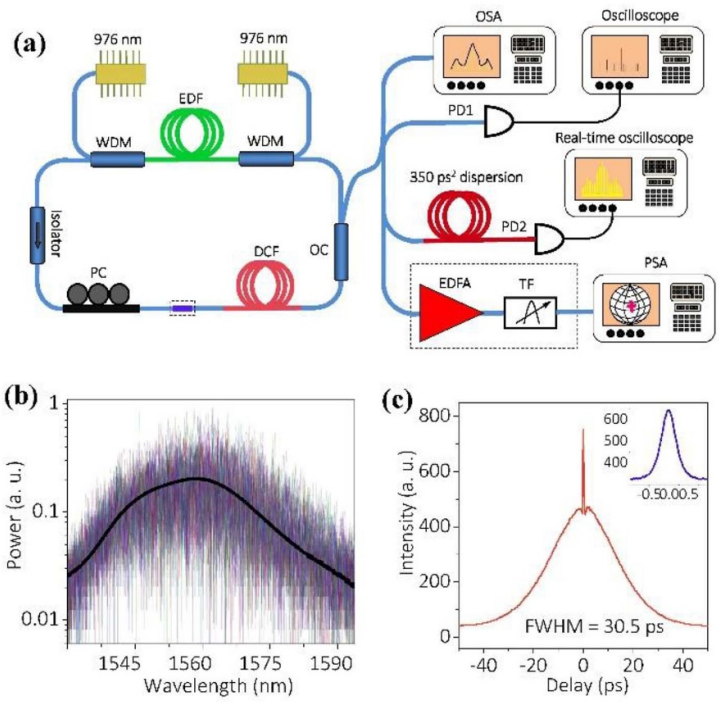

Figure 2.1. (a) Experimental setup of PML and detection method. (b) 100 single-shot spectra; the black line is the averaged spectrum. (c) Corresponding autocorrelation trace; the inset shows the coherent peak with a smaller scale (reproduced from [96]).

The autocorrelation trace in figure 2.1(c) exhibits a pedestal with a FWHM of 30.5 ps, and the coherent peak is about 416 fs.

2.2. Data and discussion

We measured the SOP of each filtered wavelength. Figures 2.2(a)–(c) show that SOPs for wavelengths far away from the center line bifurcate into a cross-like shape on the Poincaré sphere. Multiple wave mixing processes generate new frequencies with separately evolving azimuth and ellipticity angles, resulting in perpendicular lines aligning with either a meridian or a parallel curve.

SOP turbulence is accompanied by the loss of temporal coherence. Irregular SOPs located outside of the main polarization directions emerge when the pump power P exceeds 250 mW. Four-wave-mixing (FWM) cascades with nonlinear chaotic phase-matching conditions originate from nonlinear net phase shifts in the resonator. Whenever the pump power is larger than 600 mW, cascade FWM leads to a fully developed turbulent evolution with random SOPs. As depicted in figure 2.3, irregular points with distance far away from each other are observed, with abnormal probabilities. This results in a distorted Gaussian PDF. L-shaped PDFs denote the formation of PRWs, whose generation is attributed to a stochastic mixing of vector laser modes.

3. Optical polarization rogue waves in DS

3.1. DS based on carbon-nanotubes

DSs have been investigated in diverse laser systems, operating with different rare earth-doped gain media [103–105]. Figure 3.1(a) schematically depicts a typical ring cavity containing 15 m EDF and 2.7 m SMF. The SA is based on single-wall carbon nanotubes. Here, we detect the single-shot spectra by a DFT method, and also record their SOP evolution dynamics with high speed PSA.

3.2. Data and discussion

In figure 3.1(b), for pump powers smaller than 53 mW, the laser operates from random amplified spontaneous emission (ASE) into an unstable pulse regime, until it enters into a stable regime. For the unstable regime, we observe a giant CW component, located on the broadened edge of the pulsed component. By further increasing the pump power, one gradually broadens the optical spectrum. Too large gain deteriorates the mode-locking state. This deterioration can be identified from the noisy frequencies appearing in the two fronts of the optical spectrum for the pump power of 70 mW, which originate from

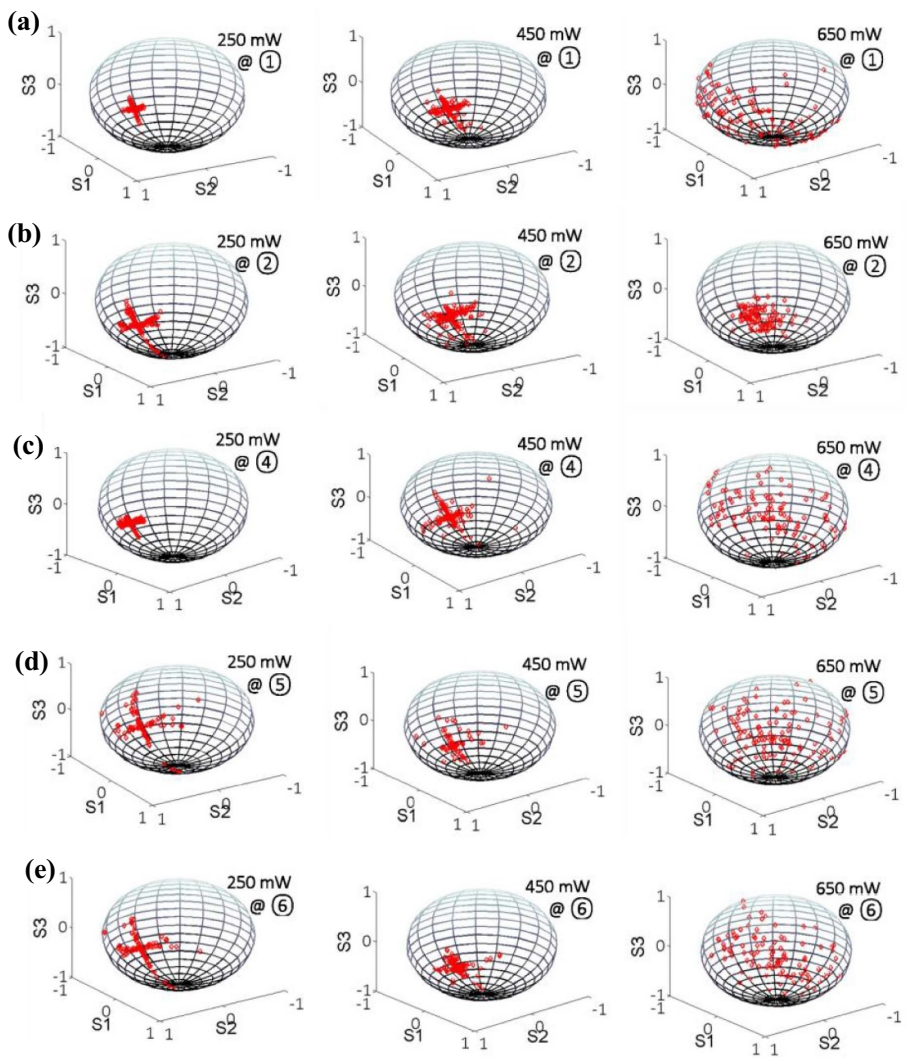

Figure 2.2. Measured SOPs for filtered wavelengths for various pump powers [96]. The filtered central wavelengths in (a)-(e) are 1547.6 nm, 1556.1 nm, 1565 nm, 1574.1 nm, 1582.7 nm, respectively.

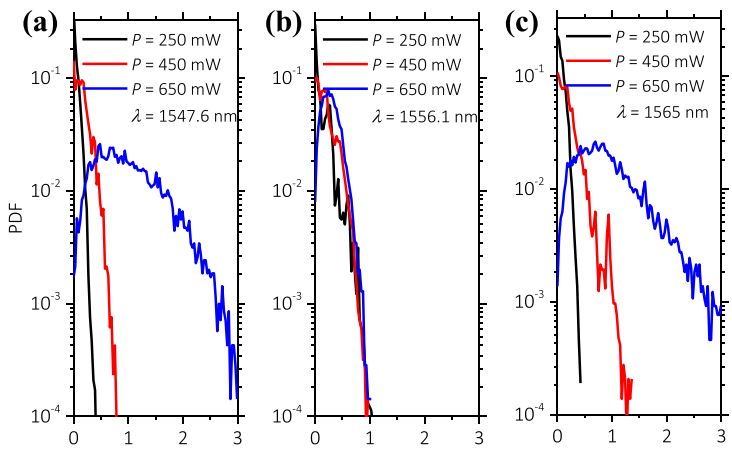

Figure 2.3. (a)–(c) Logarithm of the PDFs of the distance between each polarization point [74].

stochastic longitudinal modes mixing via the nonlinear optical response of the SA with a low saturation power.

During the formation of DSs, the optical spectrum grows broader by drawing energy from the CW component, until it decays swiftly due to insufficient cavity gain. The single-shot spectra in figure 3.2 denote

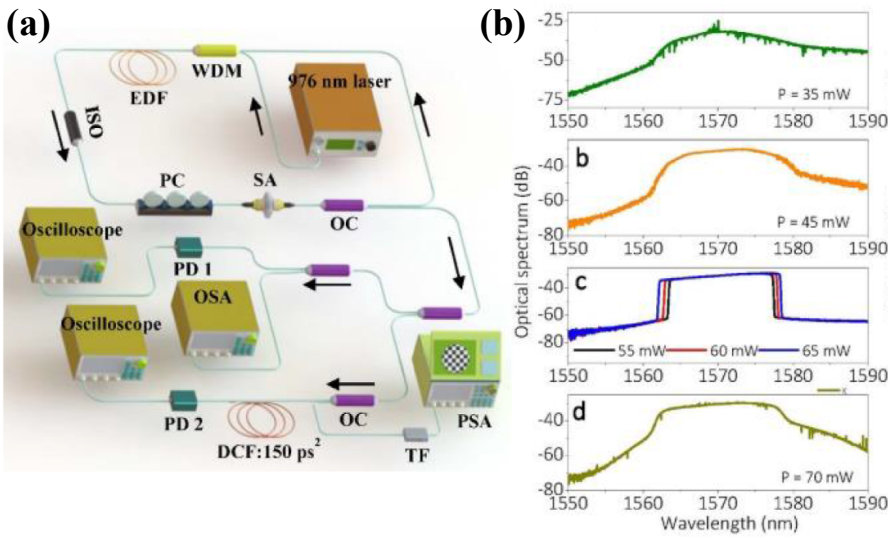

Figure 3.1. (a) Schematic of the fiber laser cavity and measurement methods. (b) Averaged optical spectra for various pump powers (reproduced from [104]).

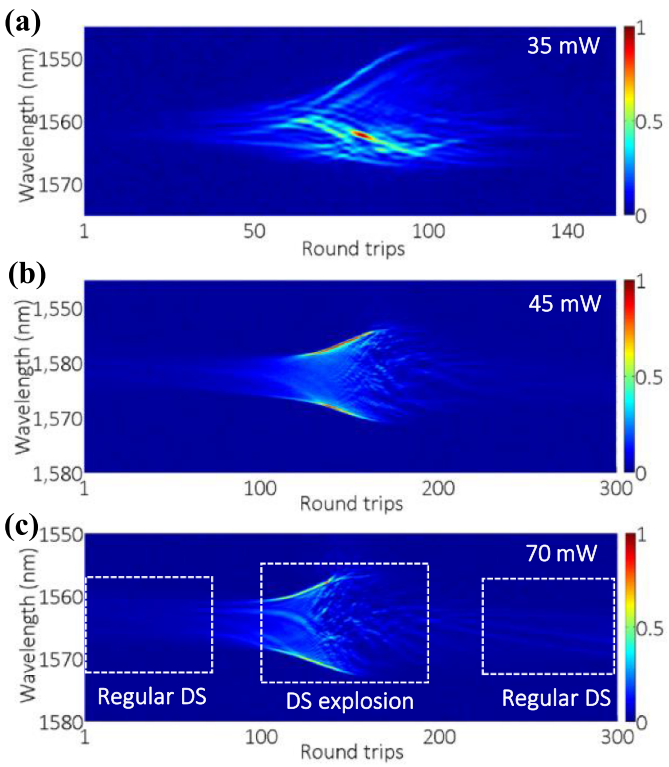

Figure 3.2. (a)–(c) Consecutive single-shot spectra in the build-up of a DS for different pump powers (reproduced from [104]).

the presence of multiple wave couplings. We can see that, for a pump power below 55 mW, optical clusters are formed, while for a pump power of 70 mW, we identify DS explosions. During DS explosions, the balance of nonlinearity, dispersion, and loss/gain is perturbed by the surplus gain at large pump powers [23, 106, 107]. Part of the DS energy dissipates into CWs via the explosion, and the DS maintains its property of being highly coherent.

The corresponding SOP evolutions give more information about the formation of DSs [24, 74, 108–111]. We measured the SOPs of different filtered wavelengths. Figure 3.3 shows that, when a DS is formed, its SOPs are evolving from a random cloud into a narrow range. Such a stable SOP structure is preserved even when its absolute value is changed, by biasing the fiber between the output OC and the PSA. During a DS

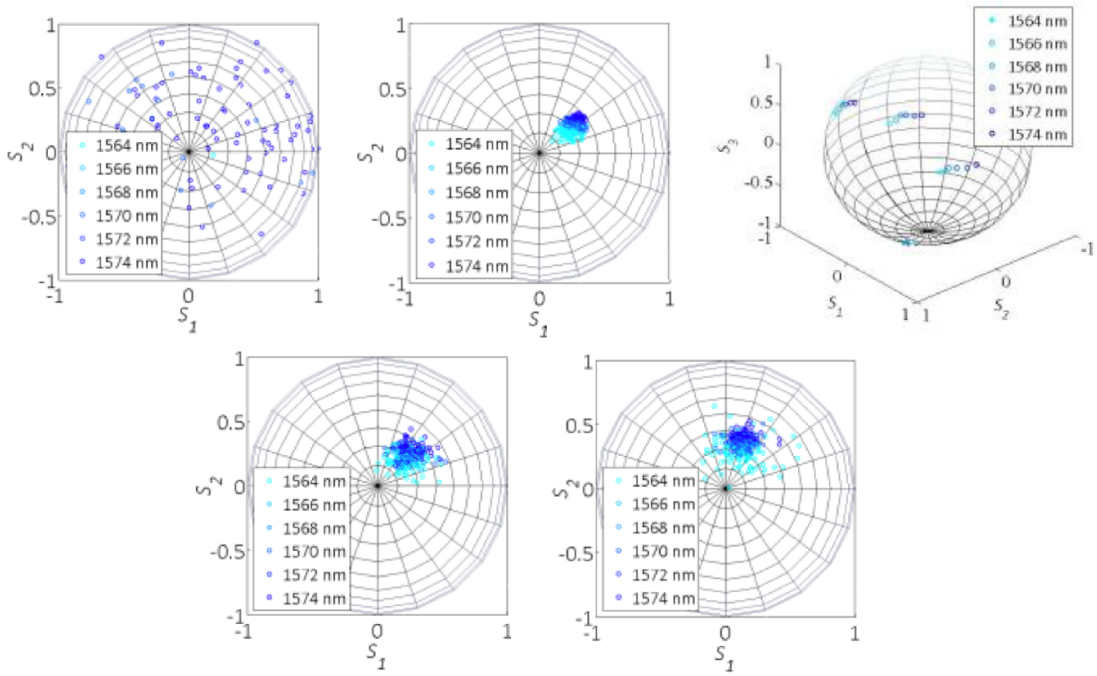

Figure 3.3. Evolution of SOPs for various filtered wavelengths and different pump powers (reproduced from [104]).

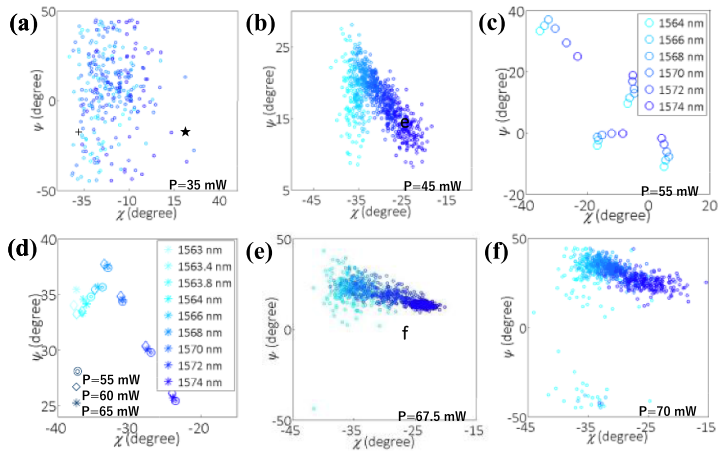

Figure 3.4. (a)–(f) Phase diagrams based on the ellipticity angle χ and spherical orientation angle ψ (reproduced from [104]).

explosion, SOPs exhibit fluctuations and tend to be spreading further on the Poincaré sphere, especially for frequencies located on the two spectral edges.

To reveal the SOP dynamics more clearly, we consider the phase diagram for the ellipticity angle χ versus the spherical orientation angle ψ:

$$\begin{cases} \chi = \dfrac{1}{2}\arctan\left(\dfrac{s_3}{\sqrt{s_1^2+s_2^2}}\right) \\ \psi = \dfrac{1}{2}\arctan\left(\dfrac{s_2}{s_1}\right). \end{cases} \tag{3.1}$$

Here, s_1, s_2, s_3 are the Stokes parameters. As shown in figure 3.4(a), the SOPs follow a random distribution, where ASE dominates. Figure 3.4(b) shows that all SOPs are located within a well-defined region, although they still behave erratically. For a stable DS, as shown in figure 3.4(c), a rectangle-shaped optical spectrum results into a fixed distribution along a folding trajectory. Whereas deteriorated distributions are observed during DS explosions, and additional frequencies with distant SOPs are detected.

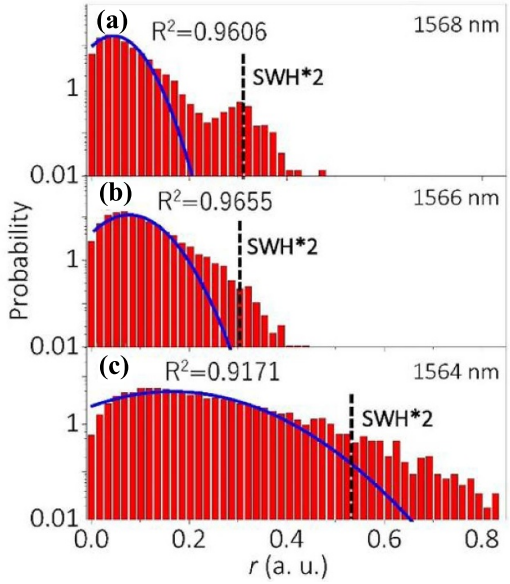

Figure 3.5. Histograms of the distance r between points on the Poincaré sphere for 70 mW pump power (reproduced from [104]).

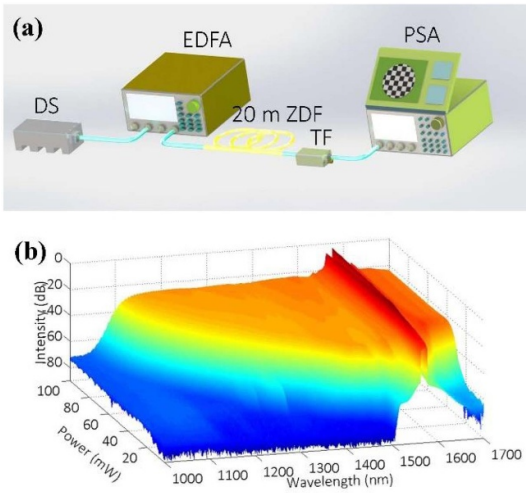

Figure 4.1. (a) The experimental setup and measurement. (b) SCG of the amplified DS (reproduced from [112]).

Figure 3.5 denotes the PDFs of r for DS explosions, where the formation of PRWs is detected. The PDF of r has a quasi-Gaussian shape in its central region. Howbeit, figure 3.5 also shows that, for wavelengths far away from the spectral center, PDFs tend to be L-shaped. From the measurement in the phase diagram, such rogue events appear with both unexpected values and relatively large probabilities of occurrence. From a statistical point of view, the occurrence of PRWs can be testified by the emergence of a heavy tail in the histogram. For example, for the r beyond the Gauss fitting, the associated probabilities are larger than twice of the SWH.

4. Optical polarization rogue waves in SCG

4.1. Experimental setup

We further identify the presence of optical PRWs in supercontinuum generation, pumped by an amplified DS, generated as described in section 3. Figure 4.1(a) depicts the experimental setup, consisting of a DS laser source, a commercial erbium-doped fiber amplifier (EDFA), and 20 m of highly nonlinear fiber (ZDF). After SCG, signal is filtered by a TF. The output SOP is detected by a high-speed PSA. After the EDFA, the average power is amplified from 0.5 mW up to 100 mW, and the pulse duration is compressed from 29 ps down to 1.5 ps.

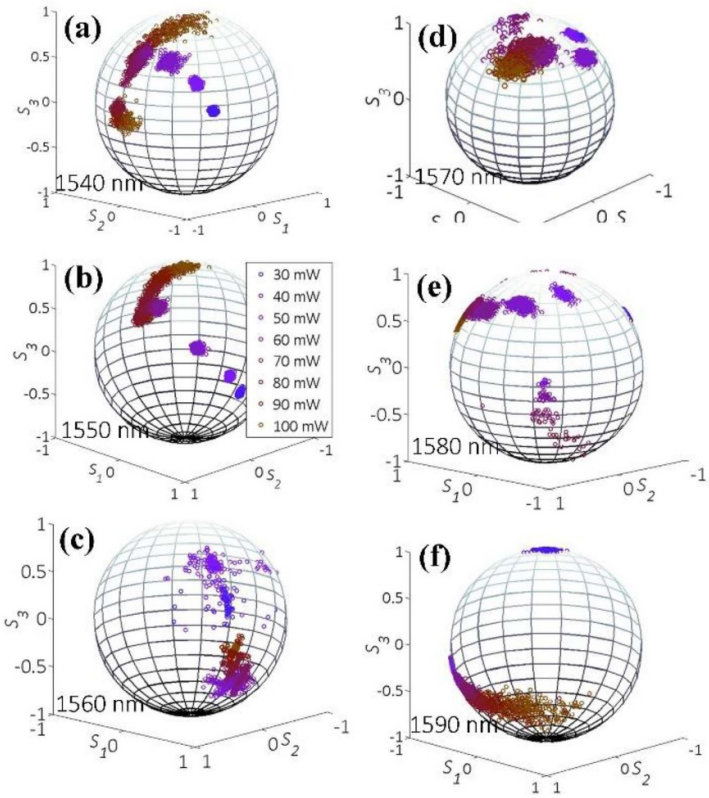

Figure 4.2. (a)–(f) SOPs for various wavelengths and pump powers. Cross-shaped lines in (c) indicate the presence of vector FWM [112].

4.2. Results and discussion

Figure 4.1(b) shows the SCG optical spectrum as a function of pump power, that increases with a step of 1 mW. The supercontinuum is rather flat after the EDFA: the 3 dB flatness in the blue side can be larger than 350 nm. We classified the SCG process in terms of two different stages: (1) the scalar stage, (2) the vector stage. For 15 mW, we observe a scalar stage, where cascaded symmetric sidebands are generated around the DS spectrum. Different orders of Stokes and anti-Stokes sidebands appear. The gain $g(\Omega)$ of the primary MI sidebands reads as

$$g(\Omega) = |\beta_2 W| \sqrt{\left(\frac{4\gamma P}{|\beta_2|} - \Omega^2\right)} \tag{4.1}$$

where, β_2, γ, and P are the group velocity dispersion (GVD), the nonlinear coefficient, and the peak power, respectively. Owing to the nominally zero GVD, sideband shifts are unusually large, and they increase with the power.

After the scalar stage, a slight interference pattern appears. For 40 mW, vector FWMs contributes to spectrum broadening, and new frequencies are generated in both forward and backward directions (that is, away from and back into the pump frequency). Eventually, a broad and flat spectrum is formed via the merging of all FWMs processes.

SOPs tends to be scattered around in the vector stage, as shown in figures 4.2(a)–(f). For pump powers larger than 30 mW, the SOPs scatter over a broad area. Meanwhile, the degree of SOP scattering increases with pump power, because of stronger FWMs. Eventually, the phases of newly generated frequencies are loosely fixed and become chaotic. This process deteriorates the coherence of SCG.

Figure 4.3 shows the PDF of r at 1570 nm, which is representative of the behavior within the spectral range of the SC. For 40 mW, the PDF is quasi-Gaussian. Whereas, when the pump power grows above 70 mW, a heavy tail appears. We identify the PRWs whenever r is larger than twice of the SWH. However, the probability to find PRWs for pump powers of 100 mW decreases unexpectedly, and the PDF returns to a Gaussian shape. The reason could be that frequencies undergo intense cascaded FWM in both forward and backward directions, and the energy coupling among different wavelengths and SOPs is rapidly varying. New frequencies with larger r are generated, while they are also annihilated.

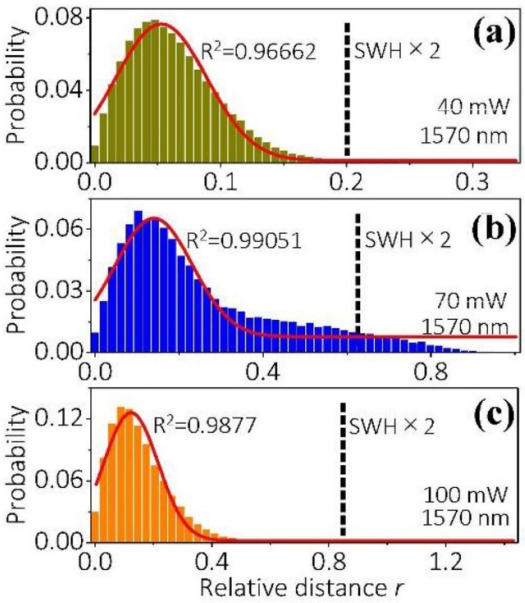

Figure 4.3. Histograms for wavelength of 1570 nm for different pump powers [112].

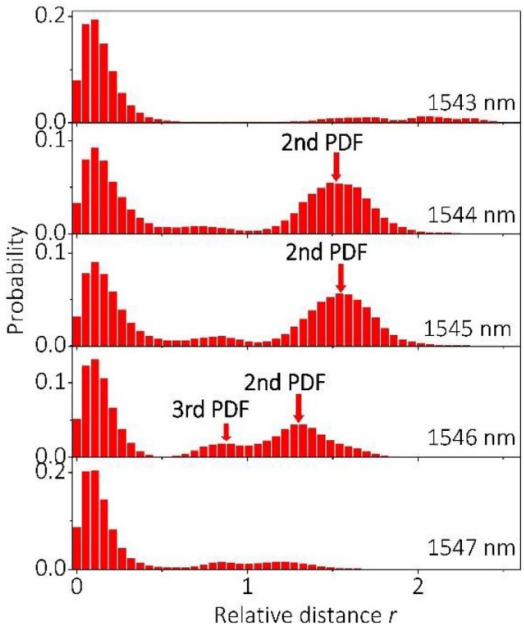

Figure 4.4. Histograms for different wavelengths between 1543 nm and 1547 nm [112].

Specifically, we may calculate the PDFs for wavelengths ranging from 1541 nm to 1557 nm in figure 4.4. SOPs emerging at 1557 nm are scattered within a single domain. For wavelengths situated farther away, the SOPs scatter within different domains. For 100 mW pumped supercontinuum, the histograms are highly sensitive to the specific filtered wavelength. For example, at 1543 nm and 1547 nm, SOPs with rogue positions are observed on the Poincaré sphere, as denoted by the heavy tails at large r values. However, double and triple PDFs may appear, depending on the wavelength that we selected.

When compared with intensity distributions for conventional RWs, PRWs in SCG are slightly different. Quantitatively, PRWs are identified on the basis of the PDF of r, while conventional RWs denote the presence of abnormally large intensities within a wide frequency range. The temporal intensities for PRWs may not be large when considering their specific generation procedure. However, we believe that there are intrinsic connections between PRWs and conventional RWs, since both waves are only formed by highly nonlinear processes.

5. Conclusion

We review recent process of studies on the polarization-dependent characteristics of optical RWs. The associated experiments show that the generation of RWs in nonlinear optical systems is generally polarization-dependent. A new statistical model based on the relative distance, r, between the SOPs of different wavelength components on the Poincaré sphere was proposed, in order to quantitatively identify the presence of PRWs. This measure permits to identify frequencies with a freak state of polarization, that is, with abnormal probabilities that deviate from a normal distribution. Next, we gave a short summary of the identification of PRWs in three nonlinear laser systems. Specifically: a partially mode-locked fiber laser, a dissipative soliton laser, and supercontinuum generation pumped by an amplified dissipative soliton. We identified the presence and properties of PRWs in those nonlinear laser systems. All of these laser systems undergo a transition from a high coherence to a low coherence regime, due to vector four-wave-mixing processes. Investigations of PRWs provide additional insight for our understanding of the nonlinear optical processes associated with the generation of RWs.

Acknowledgments

This work was financially supported by the Natural Science Foundation of China (61635004, 61405023), the National Postdoctoral Program for Innovative Talents (BX201600200), the European Research Council (ERC) under the European Union's Horizon 2020 research and innovation programme (740355), and the Russian Ministry of Science and Education (14. Y26.31.0017).

ORCID iD

Lei Gao https://orcid.org/0000-0003-2164-0480

References

[1] Kharif C and Pelinovsky E 2003 Physical mechanisms of the rogue wave phenomenon *Eur. J. Mech.* B **22** 603–34
[2] White B and Fornberg B 1998 On the chance of freak waves at sea *J. Fluid Mech.* **355** 113–38
[3] Akhmediev N and Pelinovsky E 2010 Discussion & debate: rogue waves – towards a unifying concept? *Eur. Phys. J. Spec. Top.* **185** 1–266
[4] Onorato M, Osborne A, Serio M and Bertone S 2001 Freak waves in random oceanic sea states *Phys. Rev. Lett.* **86** 5831–4
[5] Akhmediev N, Soto-Crespo J M and Ankiewicz A 2009 Extreme waves that appear from nowhere: on the nature of rogue waves *Phys. Lett.* A **373** 2137–45
[6] Dyachenko A and Zakharov V 2008 On the formation of freak waves on the surface of deep water *JETP Lett.* **88** 307–11
[7] Konotop V V, Yang J and Zezyulin D A 2016 Nonlinear waves in PT-symmetric systems *Rev. Mod. Phys.* **88** 035002
[8] Chen S, Baronio F, Soto-Crespo J M, Grelu P and Mihalache D 2017 Versatile rogue waves in scalar, vector, and multidimensional nonlinear systems *J. Phys. A: Math. Theor.* **50** 463001
[9] Dudley J M, Genty G, Mussot A, Chabchoub A and Dias F 2019 Rogue waves and analogies in optics and oceanography *Nat. Rev. Phys.* **1** 675
[10] Onorato M, Residori S, Bortolozzo U, Montina A and Arecchi F T 2013 Rogue waves and their generating mechanisms in different physical contexts *Phys. Rep.* **528** 47–89
[11] Baronio F, Conforti M, Degasperis A, Lombardo S, Onorato M and Wabnitz S 2014 Vector rogue waves and baseband modulation instability in the defocusing regime *Phys. Rev. Lett.* **113** 034101
[12] Kibler B, Chabchoub A, Gelash A, Akhmediev N and Zakharov V E 2015 Superregular breathers in optics and hydrodynamics: omnipresent modulation instability beyond simple periodicity *Phys. Rev.* X **5** 041026
[13] Fochesato C, Grilli S and Dias F 2007 Numerical modeling of extreme rogue waves generated by directional energy focusing *Wave Motion* **44** 395–416
[14] Clauss G F 2002 Dramas of the sea: episodic waves and their impact on offshore structures *Appl. Ocean Res.* **24** 147–61
[15] Brown M and Jensen A 2001 Experiments on focusing unidirectional water waves *J. Geophys. Res.* **106** 16917
[16] Yan Z, Konotop V V and Akhmediev N 2010 Three-dimensional rogue waves in nonstationary parabolic potentials *Phys. Rev.* E **82** 036610
[17] Leonetti M and Conti C 2015 Observation of three dimensional optical rogue waves through obstacles *Appl. Phys. Lett.* **106** 254103
[18] Chen S, Soto-Crespo J M, Baronio F, Grelu P and Mihalache D 2016 Rogue-wave bullets in a composite (2 +1)D nonlinear medium *Opt. Express* **24** 15251
[19] He J S, Zhang H R, Wang L H, Porsezian K and Fokas A S 2013 Generating mechanism for higher-order rogue waves *Phys. Rev.* E **87** 052914
[20] Chabchoub A, Hoffmann N, Onorato M and Akhmediev N 2012 Super rogue waves: observation of a higher-order breather in water waves *Phys. Rev.* X **2** 011015
[21] Chen S, Zhou Y, Bu L, Baronio F, Soto-Crespo J M and Mihalache D 2019 Super chirped rogue waves in optical fibers *Opt. Express* **27** 11370
[22] Baronio F, Conforti M, Degasperis A and Lombardo S 2013 Rogue waves emerging from the resonant interaction of three waves *Phys. Rev. Lett.* **111** 114101

[23] Birkholz S, Nibbering E T J, Brée C, Skupin S, Demircan A, Genty G and Steinmeyer G 2013 Spatiotemporal Rogue Events in Optical Multiple Filamentation *Phys. Rev. Lett.* **111** 243903
[24] Solli D R, Ropers C, Koonath P and Jalali B 2007 Optical rogue waves *Nature* **450** 1054
[25] Dudley J M, Dias F, Erkintalo M and Genty G 2014 Instabilities, breathers and rogue waves in optics *Nat. Photon.* **8** 755–64
[26] Lecaplain C, Grelu P, Soto-Crespo J M and Akhmediev N 2012 Dissipative rogue waves generated by chaotic pulse bunching in a mode-locked laser *Phys. Rev. Lett.* **108** 233901
[27] Liu Z, Zhang S and Wise F W 2015 Rogue waves in a normal-dispersion fiber laser *Opt. Lett.* **40** 1366
[28] Eckmann J P 1981 Roads to turbulence in dissipative dynamical systems *Rev. Mod. Phys.* **53** 643–54
[29] Bludov Y V, Konotop V V and Akhmediev N 2009 Matter rogue waves *Phys. Rev.* A **80** 033610
[30] Bludov Y V, Konotop V V and Akhmediev N 2010 Vector rogue waves in binary mixtures of Bose-Einstein condensates *Eur. Phys. J. Spec. Top.* **185** 169–80
[31] Moslem W M, Shukla P K and Eliasson B 2011 Surface plasma rogue waves *Europhys. Lett.* **96** 25002
[32] Stenflo L and Marklund M 2010 Rogue waves in the atmosphere *J. Plasma Phys.* **76** 293–5
[33] Shats M, Punzmann H and Xia H 2010 Capillary rogue waves *Phys. Rev. Lett.* **104** 104503
[34] Osborne A R, Onorato M and Serio M 2000 The nonlinear dynamics of rogue waves and holes in deep-water gravity wave trains *Phys. Lett.* A **275** 386–93
[35] Moslem W M, Sabry R, El-Labany S K and Shukla P K 2011 Dust-acoustic rogue waves in a nonextensive *Plasma Phys. Rev.* E **84** 066402
[36] Moslem W M 2011 Langmuir rogue waves in electron-positron plasmas *Phys Plasmas* **18** 032301
[37] Onorato M, Proment D and Toffoli A 2011 Triggering rogue waves in opposing currents *Phys. Rev. Lett.* **107** 184502
[38] Zhen-Ya Y 2010 Financial rogue waves *Commun. Theor. Phys.* **54** 947
[39] Akhmediev N, Dudley J M, Solli D R and Turitsyn S K 2013 Recent progress in investigating optical rogue waves *J. Opt.* **15** 060201
[40] Erkintalo M, Genty G and Dudley J M 2010 On the statistical interpretation of optical rogue waves *Eur. Phys. J. Spec. Top.* **185** 135–44
[41] Zaviyalov A, Egorov O, Iliew R and Lederer F 2012 Rogue waves in mode-locked fiber lasers *Phys. Rev.* A **85** 013828
[42] Suret P, Koussaifi R E, Tikan A, Evain C, Randoux S, Szwaj C and Bielawski S 2016 Single-shot observation of optical rogue waves in integrable turbulence using time microscopy *Nat. Commun.* **7** 13136
[43] Närhi M, Wetzel B, Billet C, Toenger S, Sylvestre T, Merolla J, Morandotti R, Dias F, Genty G and Dudley J M 2016 Real-time measurements of spontaneous breathers and rogue wave events in optical fibre modulation instability *Nat. Commun.* **7** 13675
[44] Dudley J M, Genty G and Eggleton B J 2008 Harnessing and control of optical rogue waves in supercontinuum generation *Opt. Express* **16** 3644–51
[45] Arecchi F T, Bortolozzo U, Montina A and Residori S 2011 Granularity and inhomogeneity are the joint generators of optical rogue waves *Phys. Rev. Lett.* **106** 153901
[46] Frisquet B, Kibler B, Morin P, Baronio F, Conforti M, Millot G and Wabnitz S 2016 Optical dark rogue wave *Sci. Rep.* **6** 20785
[47] D R S, Ropers C and Jalali B 2010 Rare frustration of optical supercontinuum generation *Appl. Phys. Lett.* **96** 151108
[48] Picozzi A, Garnier J, Hansson T, Suret P, Randoux S, Millot G and Christodoulides D N 2014 Optical wave turbulence: towards a unified nonequilibrium thermodynamic formulation of statistical nonlinear optics *Phys. Rep.* **542** 1–132
[49] Birkholz S, Bree C, Demircan A and Steinmeyer G 2015 Predictability of rogue events *Phys. Rev. Lett.* **114** 213901
[50] Alam M R 2014 Predictability horizon of oceanic rogue waves *Geophys. Res. Lett.* **41** 8477–85
[51] Akhmediev N, Ankiewicz A, Soto-Crespo J M and Dudley J M 2011 Rogue wave early warning through spectral measurements? *Phys. Lett.* A **375** 541–4
[52] Turitsyna E G, Smirnov S V, Sugavanam S, Tarasov N, Shu X, Babin S A, Podivilov E V, Churkin D V, Falkovich G and Turitsyn S K 2013 The laminar–turbulent transition in a fibre laser *Nat. Photon.* **7** 783–6
[53] Grossmann S 2000 The onset of shear flow turbulence *Rev. Mod. Phys.* **72** 603–18
[54] Castelvecchi D 2017 On the trail of turbulence *Nature* **548** 382–3
[55] Walczak P, Randoux S and Suret P 2015 Optical rogue waves in integrable turbulence *Phys. Rev. Lett.* **114** 143903
[56] Turitsyna E G, Falkovich G, Mezentsev V K and Turitsyn S K 2009 Optical turbulence and spectral condensate in long-fiber lasers *Phys. Rev.* A **80** 031804
[57] Ankiewicz A, Devine N and Akhmediev N 2009 Are rogue waves robust against perturbations? *Phys. Lett.* A **373** 3997–4000
[58] Kibler B, Fatome J, Finot C, Millot G, Dias F, Genty G, Akhmediev N and J M D 2010 The Peregrine soliton in nonlinear fibre optics *Nat. Phys.* **6** 790–5
[59] Dysthe K B and Trulsen K 1999 Note on breather type solutions of the NLS as models for freak-waves *Phys. Scr.* **T82** 48
[60] Akhmediev N and Ankiewicz A 1997 *Solitons: Non-linear Pulses and Beams* (London: Chapman & Hall)
[61] Tai K, Hasegawa A and Tomita A 1986 Observation of modulational instability in optical fibers *Phys. Rev. Lett.* **56** 135–8
[62] Dudley J M, Genty G and Coen S 2006 Supercontinuum generation in photonic crystal fiber *Rev. Mod. Phys.* **78** 1135–84
[63] Solli D R, Herink G, Jalali B and Ropers C 2012 Fluctuations and correlations in modulation instability *Nat. Photon.* **6** 463–8
[64] Mitchell M, Chen Z, Shih M and Segev M 1996 Self-trapping of partially spatially incoherent light *Phys. Rev. Lett.* **77** 490–3
[65] Soljacic M, Segev M, Coskun T, Christodoulides D and Vishwanath A 2000 Modulation instability of incoherent beams in noninstantaneous nonlinear media *Phys. Rev. Lett.* **84** 467–70
[66] Kip D, Soljacic M, Segev M, Eugenieva E and Christodoulides D 2000 Modulation instability and pattern formation in spatially incoherent light beams *Science* **290** 495–8
[67] Chen Z, Mitchell M, Segev M, Coskun T H and Christodoulides D N 1998 Self-trapping of dark incoherent light beams *Science* **280** 889–92
[68] Picozzi A, Haelterman M, Pitois S and Millot G 2004 Incoherent solitons in instantaneous response nonlinear media *Phys. Rev. Lett.* **92** 143906
[69] Kibler B, Michel C, Kudlinski A, Barviau B, Millot G and Picozzi A 2011 Emergence of spectral incoherent solitons through supercontinuum generation in photonic crystal fibers *Phys. Rev.* E **84** 066605
[70] Hammani K, Kibler B, Finot C and Picozzi A 2010 Emergence of rogue waves from optical turbulence *Phys. Lett.* A **374** 3585–9
[71] Kolpakov S A, Kbashi H and Sergeyev S V 2016 Dynamics of vector rogue waves in a fiber laser with a ring cavity *Optica* **3** 870–5
[72] Sergeyev S V 2014 Fast and slowly evolving vector solitons in mode-locked fibre lasers *Philos. Trans. R. Soc.* A **372** 20140006
[73] Krupa K, Nithyanandan K and Grelu P 2017 Vector dynamics of incoherent dissipative optical solitons *Optica* **4** 1239–44
[74] Gao L, Zhu T, Wabnitz S, Li Y J, Tang X S and Cao Y L 2018 Optical puff mediated laminar-turbulent polarization transition *Opt. Express* **26** 6103–13

[75] Hanson R and Awschalom D D 2008 Coherent manipulation of single spins in semiconductors *Nature* **453** 1043–9
[76] McNeil B W J and Thompson N R 2010 X-ray free-electron lasers *Nat. Photon.* **4** 814–21
[77] Avila K, Moxey D, de Lozar A, Avila M, Barkley D and Hof B 2011 The onset of turbulence in pipe flow *Science* **333** 192–6
[78] Fermann M E and Hartl I 2013 Ultrafast fibre lasers *Nat. Photon.* **7** 868–74
[79] Grelu P and Akhmediev N 2012 Dissipative solitons for mode-locked lasers *Nat. Photon.* **6** 84–92
[80] Oktem B, Ülgüdür C and Ilday F Ö 2010 Soliton–similariton fibre laser *Nat. Photon.* **4** 307–11
[81] Lecaplain C and Grelu P 2014 Rogue waves among noiselike-pulse laser emission: an experimental investigation *Phys. Rev.* A **90** 013805
[82] Runge A, Aguergaray C, Broderick N and Erkintalo M 2014 Raman rogue waves in a partially mode-locked fiber laser *Opt. Lett.* **39** 319–22
[83] Gao L, Zhu T, Liu M and Huang W 2015 Cross-phase modulation instability in mode-locked laser based on reduced graphene oxide *IEEE Photon. Technol. Lett.* **27** 38–41
[84] Smith N J and Doran N J 1996 Modulational instabilities in fibers with periodic dispersion management *Opt. Lett.* **21** 570–2
[85] Kudlinski A, Bendahmane A, Labat D, Virally S, Murray R T, Kelleher E J R and Mussot A 2013 Simultaneous scalar and cross-phase modulation instabilities in highly birefringent photonic crystal fiber *Opt. Express* **21** 8437
[86] Horowitz M, Barad Y and Silberberg Y 1997 Noiselike pulses with a broadband spectrum generated from an erbium-doped fiber laser *Opt. Lett.* **22** 799–801
[87] Zhao L M, Tang D Y, Cheng T H, Tam H Y and Lu C 2008 120 nm Bandwidth noise-like pulse generation in an erbium-doped fiber laser *Opt. Commun.* **281** 157–61
[88] Jeong Y, Vazquez-Zuniga L A, Lee S and Kwon Y 2014 On the formation of noise-like pulses in fiber ring cavity configurations *Opt. Fiber Technol.* **20** 575–92
[89] Runge A, Aguergaray C, Broderick N and Erkintalo M 2013 Coherence and shot-to-shot spectral fluctuations in noise-like ultrafast fiber lasers *Opt. Lett.* **38** 4327
[90] North T and Rochette M 2013 Raman-induced noiselike pulses in a highly nonlinear and dispersive all-fiber ring laser *Opt. Lett.* **38** 890–2
[91] Churkin D V, Sugavanam S, Tarasov N, Khorev S, Smirnov S V, Kobtsev S M and Turitsyn S K 2015 Stochasticity, periodicity and localized light structures in partially mode-locked fibre lasers *Nat. Commun.* **6** 7004
[92] Tang D Y, Zhao L M and Zhao B 2005 Soliton collapse and bunched noise-like pulse generation in a passively mode-locked fiber ring laser *Opt. Express* **13** 2289–94
[93] Wang Q Q, Chen T, Li M, Zhang B, Lu Y F and Chen K P 2013 All-fiber ultrafast thulium-doped fiber ring laser with dissipative soliton and noise-like output in normal dispersion by single-wall carbon nanotubes *Appl. Phys. Lett.* **103** 011103
[94] Peccianti M, Pasquazi A, Park Y, Little B E, Chu S T, Moss D J and Morandotti R 2012 Demonstration of a stable ultrafast laser based on a nonlinear microcavity *Nat. Commun.* **3** 765
[95] Herr T, Hartinger K, Riemensberger J, Wang C Y, Gavartin E, Holzwarth R, Gorodetsky M L and Kippenberg T J 2012 Universal formation dynamics and noise of Kerr-frequency combs in microresonators *Nat. Photon.* **6** 480–7
[96] Gao L, Zhu T, Wabnitz S, Liu M and Huang W 2016 Coherence loss of partially mode-locked fiber laser *Sci. Rep.* **6** 24995
[97] Ferdous F, Miao H, Leaird D E, Srinivasan K, Wang J, Chen L, Varghese L T and Weiner A M 2011 Spectral line-by-line pulse shaping of on-chip microresonator frequency combs *Nat. Photon.* **5** 1–2
[98] Schröder J, Vo T D and Eggleton B J 2009 Repetition-rate-selective, wavelength-tunable mode-locked laser at up to 640 GHz *Opt. Lett.* **34** 3902–4
[99] Droques M, Kudlinski A, Bouwmans G, Martinelli G and Mussot A 2012 Experimental demonstration of modulation instability in an optical fiber with a periodic dispersion landscape *Opt. Lett.* **37** 4832
[100] Finot C, Fatome J, Sysoliatin A, Kosolapov A and Wabnitz S 2013 Competing four-wave mixing processes in dispersion oscillating telecom fiber *Opt. Lett.* **38** 5361
[101] Bao Q, Zhang H, Wang Y, Ni Z, Yan Y, Shen Z X, Loh K P and Tang D Y 2009 Atomic-layer graphene as a saturable absorber for ultrafast pulsed lasers *Adv. Funct. Mater.* **19** 3077–83
[102] Sun Z, Hasan T, Torrisi F, Popa D, Privitera G, Wang F, Bonaccorso F, Basko D M and Ferrari A C 2010 Graphene Mode-Locked Ultrafast Laser *ACS Nano* **4** 803–10
[103] Kieu K, Renninger W H, Chong A and Wise F W 2009 Sub-100 fs pulses at watt-level powers from a dissipative-soliton fiber laser *Opt. Lett.* **34** 593–5
[104] Gao L, Cao Y L, Wabnitz S, Ran H Q, Kong L D, Li Y J, Huang W, Huang L G, Feng D Q and Zhu T 2019 Polarization evolution dynamics of dissipative soliton fiber laser *Photon. Res.* **7** 1331–9
[105] Tang Y, Chong A and Wise F W 2015 Generation of 8 nJ pulses from a normal-dispersion thulium fiber laser *Opt. Lett.* **40** 2361–4
[106] Akhmediev N and Ankiewicz A 2005 *Dissipative Solitons* (Berlin: Springer)
[107] Chen H J, Liu M, Yao J, Hu S, He J B, Luo A P, Xu W C and Luo Z C 2018 Buildup dynamics of dissipative soliton in an ultrafast fiber laser with net-normal dispersion *Opt. Express* **26** 2972–82
[108] Sergeyev S V, Mou C, Turitsyna E G, Rozhin A and Turitsyn S K 2014 Spiral attractor created by vector solitons *Light Sci. Appl.* **3** e131
[109] Li D, Shen D, Li L, Tang D, Su L and Zhao L 2018 Internal polarization dynamics of vector dissipative-soliton-resonance pulses in normal dispersion fiber lasers *Opt. Lett.* **43** 1222–5
[110] Kalashnikov V, Sergeyev S V, Jacobsen G, Popov S and Turitsyn S K 2016 Multi-scale polarisation phenomena *Light Sci. Appl.* **5** e16011
[111] Mou C, Sergeyev S V, Rozhin A G and Turitsyn S K 2013 Bound state vector solitons with locked and precessing states of polarization *Opt. Express* **21** 26868–75
[112] Gao L, Kong L D, Cao Y L, Wabnitz S, Ran H Q, Li Y J, Huang W, Huang L G, Liu M and Zhu T 2019 Optical polarization rogue waves from supercontinuum generation in zero dispersion fiber pumped by dissipative soliton *Opt. Express* **27** 23830–8